10.1515/astro-2017-0176

Baltic Astronomy, vol. 23, 111–122, 2014

ANGULAR MOMENTUM IN DWARF GALAXIES

A. Del Popolo[1,2]

[1] *Dipartimento di Fisica e Astronomia, University Of Catania, Viale Andrea Doria 6, 95125 Catania, Italy*

[2] *International Institute of Physics, Universidade Federal do Rio Grande do Norte, 59012-970 Natal, Brazil*

Received: 2014 June 18; accepted: 2014 July 28

Abstract. We study the "angular momentum catastrophe" in the framework of interaction among baryons and dark matter through dynamical friction. By means of Del Popolo (2009) model we simulate 14 galaxies similar to those investigated by van den Bosch, Burkert and Swaters (2001), and calculate the distribution of their spin parameters and the angular momenta. Our model gives the angular momentum distribution which is in agreement with the van den Bosch et al. observations. Our result shows that the "angular momentum catastrophe" can be naturally solved in a model that takes into account the baryonic physics and the exchange of energy and angular momentum between the baryonic clumps and dark matter through dynamical friction.

Key words: cosmology: theory, large scale structure of Universe – galaxies: formation

1. INTRODUCTION

The formation of disk galaxies is an outstanding and partially unsolved problem in astrophysics and cosmology. Disk galaxies form from the gravitational collapse of a proto-galactic gas cloud located in a dark halo (White & Rees 1978). Assuming angular momentum conservation, the gas cloud cools during the collapse and forms a disk in the center of the halo (Fall & Efstathiou 1980). In the standard model of disk formation, it is usually assumed the detailed conservation of angular momentum (Mestel 1963), adiabatic contraction (Blumenthal et al. 1986), a realistic halo profile (e.g., Mo et al. 1998), bulge formation from disk instabilities (Mo et al. 1998; van den Bosch 1998) and supernova feedback (van der Bosch et al. 2000, 2002).

The previous ideas, developed a couple of decades ago, are related to the spine of the models of disk galaxy formation (Mo et al. 1998; van den Bosch et al. 1998, 2001, 2002; Dutton et al. 2007). Nowadays, the accepted cosmological paradigm is the ΛCDM model, in which the baryonic matter constitutes only some percent of the total content of the Universe, and the matter/energy of the Universe is dominated by dark matter (DM) ($\simeq 27\%$) and dark energy ($\simeq 68\%$) (Ade et al.

2013). The ΛCDM model is supported by the large scale structure (LSS) and evolution (Komatsu et al. 2011; Del Popolo 2007, 2013, 2014a) of the Universe, by cosmic microwave background radiation and polarization spectra (Komatsu et al. 2011), by supernovae of type Ia (Amanullah et al. 2010), and the baryon acoustic oscillations (Percival et al. 2010)[1].

An important prediction of the N-body simulations of the CDM Universe is that the halos density profile is characterized by a universal functional form, the so called Navarro-Frenk-White (NFW) profile (Navarro et al. 1996, 1997). Similarly, Bullock et al. (2001) showed through N-body simulations that also the specific angular momenta (SAM) of halos have a universal profile, whose functional form is well fitted by a 2-parameter function [2]. Halos acquire angular momentum through the tidal torque of the large-scale structure on the proto-structure (Hoyle 1949; Ryden 1988; Eisenstein & Loeb 1995).

It is common to express angular momentum in terms of a spin parameter

$$\lambda = J\sqrt{E}/GM^{5/2} \tag{1}$$

where J is the total angular momentum, E is the total energy, and M is the mass of the DM halo. The spin parameter has a lognormal distribution with a maximum at $\lambda \simeq 0.035$ and 90% probability that λ is in the range 0.02–0.1 (Vivitska et al. 2002).

Semi-analytic models of disk formation in an isolated DM halo give rise to disk sizes in agreement with the sizes of the disk observed in galaxies (Mo et al. 1998). As already reported, two of the main assumptions of the quoted models are the angular momentum conservation and the halo profile obtained from simulations. The initial specific angular momentum of gas is an input parameter, obtained from typical values of the spin parameter. A good agreement between the disk size obtained in semi-analytical models with that for real galaxies, confirms that CDM halos have enough angular momentum to form disks similar to the observed ones.

While semi-analytic models obtain the correct disk size, simulations obtain too small disks and a distribution of angular momentum in disagreement with that observed in galaxies (specific angular momentum mismatch). Smooth particle hydrodynamic (SPH) simulations found that baryons have just 10% of the real angular momentum of a galaxy (Sommer-Larsen et al. 1999; Navarro & Steinmetz 2000). The quoted problem has been dubbed as the "angular momentum catastrophe" (AMC). The problem is associated with the overcooling-problem in CDM models (e.g., White & Reese 1978; White & Frenk 1991), also seen in hydrodynamical simulations.

In simulations in which feedback effects, heating the gas (e.g., UV background reionization, ram pressure, tidal heating), are not present, the cold gas forms small clumps that collapse toward the center of the system. Those clumps loose a large part of their angular momentum which is transferred to DM through DF (Navarro & Steinmetz 2000; van den Bosch et al. 2002; Governato et al. 2010). The loss process is more effective if the gas is distributed in cold and dense lumps, rather than in smooth ones (Navarro & Benz 1990). Further loss of the angular momentum

[1] The model has problems on small scales, the cosmological constant fine tuning problem (Weinberg 1989; Astashenok & Del Popolo 2012) and the "cosmic coincidence problem".

[2] For the opposite result see in Ricotti 2003; Del Popolo 2010, 2011.

is also due to an artificial viscosity term introduced in the hydrodynamical force equation, and in the internal energy equation, in order to compensate for some artifacts resulting from the discrete representation of the fluid equations, namely to avoid particle interpenetration and damp spurious oscillations in shocks (Monaghan 1992). The quoted problem can be reduced by decreasing the graininess of the mass distribution and increasing the number of particles and resolution (Mayer et al. 2008).

There are at least two solutions proposed to the problem. The first one is based on revising the cosmological model, using for example a Warm Dark Matter (WDM) model, in which the DM particles have a non-zero thermal velocity. In this case, on large scales the structure formation continues as in the CDM model, while on small scales the structures form only above a characteristic scale because the WDM particle thermal motion would smear out short-wavelength density perturbations (Sommer-Larsen & Dolgov 2001). In the WDM model, baryons are smoothly distributed, and they loose less angular momentum to DM through DF (Sommer-Larsen & Dolgov 2001).

An astrophysical solution to the problem is based on the processes that heat the gas, which entering the halo has a smooth distribution and avoids the angular momentum loss. Astrophysical mechanisms that can heat the gas are: the injection of energy by supernovae explosions (e.g., Sommer-Larsen et al. 1999) and the radiation field produced by stars or accreting black holes. However, even if the feedback can avoid the loss of angular momentum, other problems remain like the mismatch of the angular momentum profiles (e.g., van den Bosch et al. 2001 (VBS)), or the fact that the scatter of the spin parameter of real galaxies is smaller than that in simulations (de Jong & Lacey 2000).

Maller & Dekel (2002) proposed a model in which DM distribution is different from that of gas, due to gas processes. In this model, SF removes gas from small incoming halos (giving rise to the low angular momentum component of the system) eliminating baryons with low specific angular momentum (see also Sommer-Larsen et al. 2003; Abadi et al. 2003). However, feedback models even in the absence of substructures, and then DF, have problems in forming bulgeless galaxies (van den Bosch et al. 2002), unless there exists 'selective outflows' of the low angular momentum gas (D'Onghia & Burkert 2004).

The third possibility, is that in the simulations of baryon clumps the numerical methods used can produce an artificial loss of the angular momentum. Nowadays, the solution to the AMC problem is related to the second and third issue: (a) heating of gas, and (b) improving the numerical methods and increasing the resolution (Mayer et al. 2008).

Governato et al. (2010) showed that the bulgeless galaxies with a baryonic angular momentum close to that observed in the real galaxies is obtained in SPH simulations which take account the outflows from supernovae explosions removing the gas of low angular momentum.

The gas outflows have been invoked to solve other small-scale problems of the ΛCDM model, like the cusp/core problem (Moore 1994; Flores & Primak 1994). The last is the discrepancy among the cuspy density profiles obtained in simulations (Navarro et al. 1996, 1997, 2010) and the cored density profiles observed (Burkert 1995; Del Popolo (2009) (DP09); Del Popolo & Kroupa 2009; Cardone et al. 2011; Del Popolo 2012a,b (DP12a, DP12b); Cardone & Del Popolo 2012; Del Popolo, Cardone & Belvedere 2013; Del Popolo & Hiotelis 2014; Kuzio

de Naray & Kaufmann 2011).

The previous problems can be also solved through another mechanism, namely the transfer of energy and angular momentum from the baryonic clumps to DM through a dynamical friction (El-Zant et al. 2001, 2004; Romano-Diaz et al. 2008, 2009; Del Popolo 2009; Del Popolo & Hiotelis 2014; Del Popolo et al. 2014; Cole et al. 2011; Inoue & Saitoh 2011).

In the present paper we will study if the second mechanism envisaged, i.e. the baryonic clump interaction with DM, can solve the AMC. The paper is organized as follows. In Section 2 we summarize the model. Section 3 describes the results and discussion. Section 4 is devoted to conclusions.

2. SOLVING THE ANGULAR MOMENTUM CATASTROPHE

In order to see if the interaction between the baryonic clumps and DM through a dynamical friction (El-Zant et al. 2001, 2004; Romano-Diaz et al. 2008, 2009; Del Popolo 2009; Cole et al. 2011) are able to modify the spin parameter distribution and the angular momentum distribution in a system made of baryons and DM, we use the model introduced in DP09.

2.1. Structure formation model

Here we summarize the model used to follow the structure from the linear phase to the present epoch, widely discussed in Del Popolo (2009) (DP09) (see also Del Popolo 2002; Del Popolo & Hiotelis 2014; Hiotelis & Del Popolo 2006, 2013; Cardone et al. 2011; Del Popolo 2014b).

The model described in DP09 (also in DP12a,b), is an improved spherical infall model (SIM) already discussed by several authors (Gunn & Gott 1972; Ryden & Gunn 1987 (RG87); Le Delliou & Henriksen 2003; Del Popolo, Pace & Lima 2013a,b; Del Popolo et al. 2013). Differently from previous SIMs, the adiabatic contraction, dynamical friction (DF), random angular momentum, ordered angular momentum[3], gas cooling, and star formation (see DP09; Del Popolo & Gambera 1997, 1999, 2000; Del Popolo 2014b) are all simultaneously taken into account. In the quoted model, the galaxy formation starts in a proto-structure, made of DM and gas, in its linear phase.

The initial perturbation is divided into mass shells of initial comoving radius x_i which expand to a maximum radius x_m (named turn-around radius, $x_{\rm ta}$).

The final density profile can be obtained in terms of the density at turn-around, $\rho_{\rm ta}(x_m)$, the collapse factor[4], and the turn-around radius (Eq. A18, Del Popolo 2009), as:

$$\rho(x) = \frac{\rho_{\rm ta}(x_m)}{f^3}\left[1 + \frac{d\ln f}{d\ln x_m}\right]^{-1} \tag{2}$$

In our model, the proto-structure is being formed around peaks of the density field[5], we took into account the presence of baryons, baryons' adiabatic collapse,

[3] The ordered angular momentum originates from tidal torques, while the random angular momentum originates from random motions and velocities in the collapse.

[4] The collapse factor is defined as $f = x/x_m$ (see Del Popolo 2009, Appendix A)

[5] The density profile of a proto-halo is taken to be the profile of a peak in a density field described by the Bardeen et al. (1986) power spectrum, as is illustrated in Del Popolo (2009), Figure 6.

dynamical friction and angular momentum. These quantities can be specified as we describe in the following.

The baryonic fraction is fixed following McGaugh et al. (2010). More precisely, we use the detected baryonic fraction, $f_d = (M_b/M_{500})/f_b = F_b/f_b$, which is the ratio of the actual baryon fraction, $F_b = M_b/M_{500}$, in the structure, to the amount of baryons expected from the cosmic baryon fraction, $f_b = 0.17 \pm 0.01$ (Komatsu et al. 2009). During infall, baryons compress the DM (adiabatic contraction (AC)), and are then subject to radiative processes, giving rise to clumps which condense into stars as described in Li et al. (2010) (Sect. 2.2.2, 2.2.3), De Lucia & Helmi (2008). Infalling baryon clumps suffer DF from DM particles, transferring energy and angular momentum to DM which thus moves towards the external parts of the structure and gives rise to the observed density profile flattening.

The ordered angular momentum, h, (RG87) which arises from tidal torques experienced by proto-halos, is obtained by integrating the torque over time (Ryden 1988, Eq. 35) (see Appendix C of DP09), while the random angular momentum, $j_{\rm rand}$, (RG87) which is connected to random velocities, was assigned to proto-structures according to Avila-Reese et al. (1998) scheme[6]. Dynamical friction was taken into account by introducing the dynamical friction force in the equation of motion (see DP09, Eq. A16).

The adiabatic contraction was taken into account by means of Gnedin et al. (2004) model and Klypin et al. (2002) model taking also account of exchange of angular momentum between baryons and dark matter (see appendix E of Del Popolo 2009 for a wider description), and calculated solving recursively the equation involved (Spedicato et al. 2003).

Using the DP09 model, we will follow the formation of 14 dwarfs, with the same characteristics of those studied by VBS.

2.2. Calculation of the angular momentum distribution

A virialized halo made of baryonic matter and DM of virial mass $M_{\rm vir}$ has a total specific angular momentum (SAM), $j_{\rm tot} = h + j_{\rm rand} = L_{\rm tot}/M$, L being the angular momentum, proportional to the maximum SAM, $j_{\rm max}$, and the normalized cumulative distribution, $m(j)$

$$j_{\rm tot} = j_{\rm max}\left[1 - \int_0^1 m(k){\rm d}k\right], \tag{3}$$

where $k = j/j_{\rm max}$, and

$$m(j) = \int_0^j p(j)dj, \tag{4}$$

$p(j)dj$ being the mass fraction having SAM in the j-$j + dj$ range. A quantity often used to express the angular momentum, L of a structure, is the spin parameter

$$\lambda = L\sqrt{|E|}/GM^{5/2}, \tag{5}$$

[6] This consists in expressing the specific angular momentum $j_{\rm rand}$ through the ratio $e_0 = \left(\frac{r_{\rm min}}{r_{\rm max}}\right)_0$, where $r_{\rm min}$ and $r_{\rm max}$ are the maximum and minimum penetration of the shell toward the center, respectively, and left this quantity as a free parameter (see Appendix C of DP09).

Table 1. Properties of VBS dwarf galaxies. Column (1) lists the UGC number of the galaxy. Columns (2) and (3) list $c_{\rm vir}$ and $V_{\rm vir}$ (in km/s) of the best-fit mass model, respectively. Columns (4) and (5) list the disk mass fraction $f_{\rm disk}$ and the gas mass fraction $f_{\rm gas}$, respectively. Column (6) lists the baryonic spin parameter $\lambda_{\rm disk}$, and columns (7) and (8), list the total and maximum specific angular momentum of the baryons (both in kpc/km/s).

UGC	$c_{\rm vir}$	$V_{\rm vir}$	$f_{\rm disk}$	$f_{\rm gas}$	$\lambda_{\rm disk}$	$j_{\rm tot}$	$j_{\rm max}$
731	17.6	48.6	0.024	0.801	0.061	308	775
3371	10.6	65.5	0.018	0.715	0.056	569	1618
4325	33.0	48.6	0.037	0.541	0.074	328	971
4499	2.4	126.3	0.003	0.672	0.007	330	1195
6446	9.1	56.2	0.041	0.570	0.052	397	1325
7399	19.9	65.8	0.012	0.691	0.044	396	1692
7524	6.4	78.8	0.012	0.500	0.025	393	1025
8490	17.5	53.2	0.026	0.769	0.062	378	1106
9211	19.2	41.2	0.055	0.865	0.107	381	1058
11707	14.6	62.2	0.062	0.770	0.103	886	2046
11861	16.4	93.1	0.068	0.405	0.099	1861	4820
12060	31.1	42.8	0.102	0.710	0.168	582	1477
12632	16.5	47.8	0.033	0.760	0.078	387	976
12732	9.0	68.9	0.040	0.869	0.081	926	2267

(Peebles 1969), where E indicates the system internal energy. For practical reasons, the previous spin parameter definition is substituted by

$$\lambda = \frac{j_{\rm tot}}{\sqrt{2}\, r_{\rm vir} V_{\rm vir}}, \tag{6}$$

where $V_{\rm vir} = \sqrt{GM_{\rm vir}/r_{\rm vir}}$, and $r_{\rm vir}$ is the virial radius. For a NFW profile, $\lambda' = \lambda/\sqrt{f_c}$, and f_c is a function of the concentration parameter $c_{\rm vir}$ (Mo et al. 1998).

In their study, VBS fitted the rotation curves of 14 dwarfs (previously studied by van den Bosch & Swaters 2001), assuming that the galaxies are constituted by a NFW dark halo, a thin gas disk, and a thick stellar disk. They obtained (see Tab. 1) the concentration parameter, $c_{\rm vir}$, the virial velocity, $V_{\rm vir}$, $f_{\rm disk} = M_{\rm disk}/M_{\rm vir}$, and $f_{\rm gas} = M_{\rm gas}/M_{\rm vir}$, for the 14 dwarf galaxies. Using the galaxies characteristics they found, as discussed in the following, their spin parameter distribution, and their AMD distribution.

The SAM distribution was obtained through $m(j) = M_{\rm disk}(r)/M_{\rm disk}(r_{\rm max})$, where $j = rV_c(r)$. By means of Eq. (3) they got $j_{\rm tot}$ for each galaxy and from this the disk spin parameter

$$\lambda_{\rm disk} = \frac{j_{\rm tot}}{\sqrt{2}\, r_{\rm vir} V_{\rm vir}}, \tag{7}$$

Finally, they compared the histograms of $\lambda_{\rm disk}$ distribution for the quoted galaxies with the λ distribution of DM halos (that they found in agreement, in contrast to Maller & Dekel 2002 and Governato et al. 2010), and the j distribution , $p(j)$, that was compared to the DM distribution. In their analysis, they assumed that

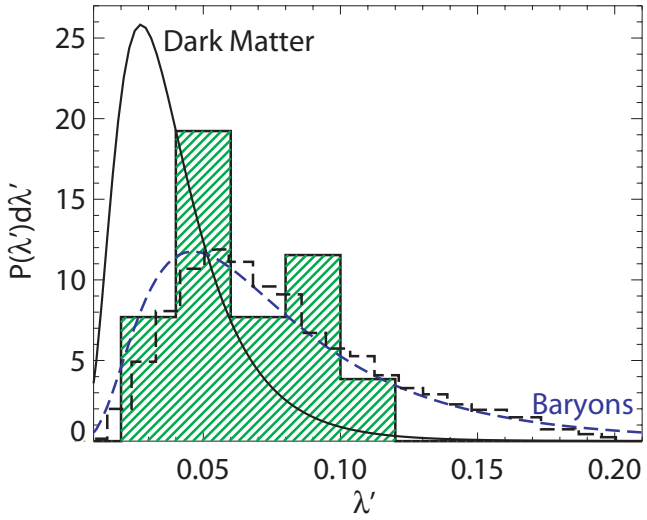

Fig. 1. The λ' distribution in the VBS sample of dwarf galaxies (shaded histogram). The dashed curve is the Maller & Dekel (2002) prediction for the baryons in dwarf galaxies (dashed curve), while the solid curve is the N-body simulation result for dark halos by Bullock et al. (2001). The dashed histogram represents our result.

the mass-to-light ratio was 1 in the R band[7].

We repeated their analysis as follows. We used the gas fraction, total SAM, obtained by them, and estimated the mass of each galaxy from their $V_{\rm vir}$, assuming that the density profile was a NFW one[8]. Then, by means of the model in Sect. 2, similarly to DP12a, we "simulated" each galaxy. Then, similarly to VBS we obtained the spin parameter distribution, and the j distribution. Improved results could be obtained using the van den Bosch & Swaters (2001) rotation curve data, and use a Burkert profile for the DM halo.

Like them, we calculated the cumulative AMD, $m(j) = M_{\rm disk}(r)/M_{\rm disk}(r_{\rm max})$, we got through Eq. (3) $j_{\rm tot}$, and then the spin parameter. Finally, we obtained the $p(j)$ of the AMDs.

3. RESULTS

The results are reported in Fig. 1 and Fig. 2. In Fig. 1 we plotted the λ' distribution. The solid line represents the results of Bullock et al. (2001) for the DM spin parameter distribution, while the dashed curve is the spin parameter distribution for baryons in the 14 galaxies obtained by Maller & Dekel (2002). The solid histogram is the spin distribution obtained from the 14 galaxies (see Maller & Dekel 2002), and the dashed histogram is the spin parameter distribution obtained from the 14 galaxies, using the method of this paper.

The plot shows that the spin distribution of DF (solid line) is different from that of galaxies (solid histogram). The spin distribution obtained by Maller & Dekel (2002) (dotted curve), and by us (dashed histogram), are in good agreement

[7] In any case, the results are not sensitive to this choice, since dwarfs are DM dominated.

[8] For a NFW profile, the virial mass is given by $M_v = \sqrt{\frac{3}{800\pi\rho_c G^3}} V_v^3 = \sqrt{1/100}(H_0 G)^{-1} V_v^3$.

with the observational distribution of the spin parameter in galaxies. The Maller & Dekel (2002) feedback model produces a good agreement with observations.

In Fig. 2 we plot the j profile for UGC 6446 obtained by VBS (right panel), and that calculated by us (left panel). The solid line is the Bullock et al. (2001) average DM j-profile while the shaded area represents the $p(j)$ of AMD for UCG 6446. The figure shows the angular-momentum profile mismatch. The dwarf angular momentum shows a deficit of angular momentum at the high and low end of the distribution, with respect to the DM distribution. In the models of Maller & Dekel (2002), or simulations of Governato et al. (2010) the low-j tail in the distribution is missing because feedback (blowout) selectively removes gas from small satellites, giving rise to the material of the halo having low-j. The bottom panel in Fig. 2 is the result obtained from Governato et al. (2010) through SPH simulations.

In our model, the reduction of DM density in the inner part of halos (previously described) and the change of the angular momentum distribution are due to the complex interplay of baryons and DM which acts similarly to the feedback mechanism in Maller & Dekel (2002) and Governato et al. (2010).

The differences among the predicted distribution of the angular momentum in our model and in N-body simulations has already been discussed in DP09 (Sect. 3). As already has been written, the differences are due to the baryon DM interplay, not considered in purely N-body simulations.

In our semi-analytic model, structure formation undergoes quiescent accretion, and minor mergers, differently from simulations in which the structures are obtained as a result of major mergers of sub-halos. The existence of many spiral galaxies with thin disks somehow supports the previous quiescent formation mechanism. Moreover, Dekel et al. (2009), argued that disk galaxies at high z are not formed through galactic mergers, but by smooth accretion flows. Consequently, the angular momentum loss to which simulations are exposed, is not present.

In DP09 (Fig. 2), we showed that if we use our model to re-obtain a NFW profile, the angular momentum distribution is similar to that coming out from N-body simulations, namely more centrally concentrated, and in disagreement with observations. The angular momentum distribution obtained for a typical halo coming out from our model has a different distribution, as previously described in this subsection. Similarly to what happened with the semi-analytic model previously cited (e.g., Mo et al. 1998), halos and galaxies forming in our model are closer to real halos and galaxies than those generated in simulations, at least closer than those generated in the simulations some years ago. As previously reported, recently, increasing the resolution and properly using feedback, simulations are able to form realistic galaxies (e.g., Mayer et al. 2008; Governato et al. 2010). Another important issue in the solution of the angular momentum catastrophe in our model is the fact that the angular momentum is mainly lost from the smaller baryonic clumps.

As reported in DP09 (Sec. 3.1), the ordered angular momentum acquired by a halo is anticorrelated with the peak height ν (see Del Popolo & Gambera 1996), and consequently smaller halos acquire larger angular momentum. Similarly, the random angular momentum is anticorrelated with ν (see eq. (C13) and Figure 8 in DP09). Consequently, smaller baryonic clumps inside the halo have larger angular momentum (random angular momentum) than larger clumps. In the virialization process, these clumps loose more angular momentum than larger clumps,

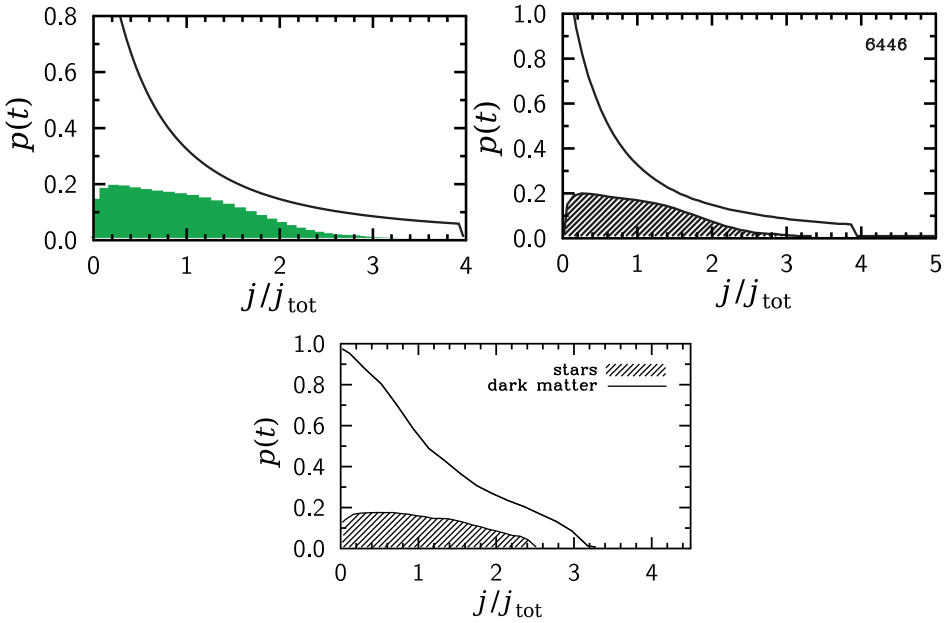

Fig. 2. The AMDs for the 14 galaxies of VBS (shaded area) compared to the median of the ΛCDM halo AMDs (solid line). In the left panel, we plot the result of our calculation, while in the right panel the VBS result for UGC 6446 is shown. The bottom panel is the result obtained by Governato et al. (2010) through SPH simulations.

explaining why the low tail in the AMD is missing in Fig. 2.

4. CONCLUSIONS

In the present paper we studied the angular momentum catastrophe in the framework of interaction among baryons and dark matter through dynamical friction (El-Zant et al. 2001, 2004; Romano-Diaz et al. 2008, 2009; DP09; Cole et al. 2011). We followed the proto-structure evolution with the DP09 semi-analytical model taking into account the effect of adiabatic contraction, dynamical friction and the exchange of angular momentum between baryons and DM, ordered and random angular momentum.

The model applied in DP09 and DP12a,b has already shown that the angular momentum got by the system through tidal torques and random velocities (random angular momentum), can be transferred in part to the DM from baryons through DM action. This produces flattening of the cusp in agreement with previous studies based on the DF driven flattening (El-Zant et al. 2001, 2004; Romano-Diaz et al. 2008) and the SF driven flattening (Navarro et al. 1996; Mashchenko et al. 2006, 2008).

Then we used our model to simulate 14 dwarfs having the same characteristics as those studied in VBS, and we calculated the distribution of the spin parameter and the AMD for the quoted dwarfs using our model.

The result of the comparison of the distribution of the spin parameter, and the angular momentum distribution, obtained from our model, to those obtained for 14 dwarfs by VBS shows that the DM and baryon distribution is different,

and we do not observe the lost of angular momentum typical in many past SPH simulations.

The solution of the angular momentum catastrophe in our model is somehow similar to that proposed by Governato et al. (2010). In their case outflows from supernovae explosions remove selectively low angular momentum gas from the system.

In our case, smaller clumps loose more angular momentum than larger clumps, explaining why the low tail in the AMD is missing.

ACKNOWLEDGMENTS. Thanks are due to the International Institute of Physics in Natal for the facilities and hospitality.

REFERENCES

Abadi M. G., Navarro J. F., Steinmetz M., Eke V. R. 2003, ApJ, 591, 499
Ade P. A. R., Aghanim N., Armitage-Caplan C. et al. 2013, arXiv:1303.5076v2
Amanullah R., Lidman C., Rubin D. et al. 2010, ApJ, 716, 712
Astashenok A. V., Del Popolo A. 2012, Class. Quant. Grav., 29, 085014 [arXiv:1203.2290]
Avila Reese V., Firmani C., Hernandez X. 1998, ApJ, 505, 37
Bardeen J. M., Bond J. R., Kaiser N., Szalay A. S. 1986, ApJ, 304, 15
Blumenthal G. R., Faber S. M., Flores R., Primack J. R. 1986, ApJ, 301, 27
Bullock J. S., Dekel A., Kolatt T. S. et al. 2001, ApJ, 555, 240
Burkert A. 1995, ApJ, 447, L25
Cardone V. F., Del Popolo A. 2012, MNRAS, 427, 3176
Cardone V. F., Del Popolo A., Tortora C., Napolitano N. R. 2011, MNRAS, 416, 1822
Cardone V. F., Leubner M. P., Del Popolo A. 2011, MNRAS, 414, 2265
Cole D. R., Dehnen W., Wilkinson M. I. 2011, MNRAS, 416, 1118
D'Onghia E., Burkert A. 2004, ApJ 612, 13
Dekel A., Birnboim Y., Engel G. et al. 2009, Nature, 457, 451
de Jong R. S., Lacey C., 2000, ApJ, 545, 781
De Lucia G., Helmi A., 2008, MNRAS, 391, 14
Del Popolo A. 2002, MNRAS, 337, 529
Del Popolo A. 2007, Astron. Rep., 51, 169
Del Popolo A. 2009, ApJ, 698, 2093
Del Popolo A. 2010, MNRAS, 408, 1808
Del Popolo A. 2011, JCAP, 07, 014
Del Popolo A. 2012a, MNRAS, 424, 38
Del Popolo A. 2012b, MNRAS, 419, 971
Del Popolo A. 2013, AIP Conf. Proc., 1548, 2
Del Popolo A. 2014a, Int. J. Mod. Phys. D, 23, 1430005
Del Popolo A. 2014b, Baltic Astronomy, 23, 55
Del Popolo A., Cardone V. F., Belvedere G. 2013, MNRAS, 429, 108
Del Popolo A., Gambera M. 1996, A&A, 308, 373
Del Popolo A., Gambera M. 1997, A&A, 321, 691
Del Popolo A., Gambera M. 1999, A&A, 344, 17
Del Popolo A., Gambera M. 2000, A&A, 357, 809

Del Popolo A., Hiotelis N. 2014, JCAP, 01, 047
Del Popolo A., Kroupa P. 2009, A&A, 502, 733
Del Popolo A., Pace F., Lima J. A. S. 2013a, MNRAS, 430, 628
Del Popolo A., Pace F., Lima J. A. S. 2013b, Int. J. Mod. Phys. D, 22, 1350038
Del Popolo A., Pace F., Maydanyuk S. P. et al. 2013, Phys. Rev. D, 87, 043527
Dutton A., van den Bosch F. C., Frank C. et al. 2007, ApJ, 654, 27
Eisenstein D. J., Loeb A. 1995, ApJ, 439, 250
El-Zant A. A., Hoffman Y., Primack J. et al. 2004, ApJ, 607, L75
El-Zant A., Shlosman I., Hoffman Y. 2001, ApJ, 560, 636
Fall S. M., Efstathiou G. 1980, MNRAS, 193, 189
Flores R. A., Primack J. R. 1994, ApJ, 427, L1
Gnedin O. Y., Kravtsov A. V., Klypin A. A., Nagai D. 2004, ApJ, 616, 16
Governato F., Brook C., Mayer L. et al. 2010, Nature, 463, 203
Gunn J. E., Gott J. R. 1972, ApJ, 176, 1
Hiotelis N., Del Popolo A. 2006, Ap&SS, 301, 167
Hiotelis N., Del Popolo A. 2013, MNRAS, 436, 163
Hoyle F. 1949, in *Problems of Cosmological Aerodynamics*, IAU and International Union of Theorethical and Applied Mechanics Symposium, eds. Burger J. M., van der Hulst H. C., Ohio, p. 195
Inoue S. Saitoh T. R. 2012, MNRAS, 422, 1902
Klypin A., Zhao H. S., Somerville R. S. 2002, ApJ, 573, 597
Komatsu E., Dunkley J., Nolta M. R. et al. 2009, ApJS, 180, 330
Komatsu E., Smith K. M., Dunkley J. et al. 2011, ApJS, 192, 18
Kuzio de Naray R., Kaufmann T. 2011, MNRAS, 414, 3617
Le Delliou M., Henriksen R. N. 2003, A&A, 408, 27
Li Y.S., De Lucia G., Helmi A. 2010, MNRAS, 401, 2036
Maller A. H., Dekel A. 2002, MNRAS, 335, 487
Mashchenko S., Couchman H. M. P., Wadsley J. 2006, Nature, 442, 539
Mashchenko S., Wadsley J., Couchman H. M. P. 2008, Science, 319, 174
Mayer L., Governato F., Kaufmann T. 2008, Adv. Sci. Lett, 1, 7
Mestel L. 1963, MNRAS, 126, 55
Mo H. J., Mao S., White S. D. M. 1998, MNRAS, 295, 319
Monaghan J. J. 1992, ARA&A, 30, 543
Moore B. 1994, Nature, 370, 629
Navarro J. F., Benz W. 1990, ApJ, 380, 320
Navarro J. F., Frenk C. S., White S. D. M. 1996, ApJ, 462, 563
Navarro J. F., Frenk C. S., White S. D. M. 1997, ApJ, 490, 493
Navarro J. F., Ludlow A., Springel V. et al. 2010, MNRAS, 402, 21
Navarro J. F., Steinmetz M. 2000, ApJ, 538, 477
Percival W. J., Reid B. A., Eisenstein D. J. et al. 2010, MNRAS, 401, 2148
Ricotti M. 2003, MNRAS, 344, 1237
Romano-Diaz E., Shlosman I., Heller C., Hoffman Y. 2009, ApJ, 702, 1250
Romano-Diaz E., Shlosman I., Hoffman Y., Heller C. 2008, ApJ, 685, L105
Ryden B. S. 1988, ApJ, 329, 589
Ryden B. S., Gunn J. E. 1987, ApJ, 318, 15
Sommer-Larsen J., Dolgov A. 2001, ApJ, 551, 608

Sommer-Larsen J., Gelato S., Vedel H. 1999, ApJ, 519, 501
Sommer-Larsen J., Gotz M., Portinari L. 2003, ApJ, 596, 47
Spedicato E., Bodon E., Del Popolo A., Mahdavi-Amiri N. 2003, 4OR, Vol. 1, Issue 1, 51
van den Bosch F. C. 1998, ApJ, 507, 601
van den Bosch F. C. 2001, MNRAS, 327, 1344
van den Bosch F. C. 2002, MNRAS, 332, 456
van den Bosch F. C., Abel T., Croft R. A. C. et al. 2002, ApJ, 576, 21
van den Bosch F. C., Burkert A., Swaters R. A. 2001, MNRAS, 326, 1205 (VBS)
van den Bosch F. C., Robertson B. E., Dalcanton J. J., de Blok W. J. G. 2000, AJ, 119, 1579
van den Bosch F. C., Swaters R. A. 2001, MNRAS, 325, 1017 (VS)
Vivitska M., Klypin A. A., Kravtsov A. V. et al. 2002, ApJ, 581, 799
Weinberg S. 1989, Rev. Mod. Phys., 61, 1
White S. D. M., Rees M. J. 1978, MNRAS, 183, 341
White S. D. M., Frenk C. S. 1991, ApJ, 379, 52